An Evaluation of Antarctic Sea Ice Thickness from the Global Ice-Ocean Modeling and Assimilation System based on In-situ and Satellite Observations

Sutao Liao[1], Hao Luo[1], Jinfei Wang[1], Qian Shi[1], Jinlun Zhang[2], Qinghua Yang[1]

[1]School of Atmospheric Sciences, Sun Yat-sen University, and Southern Marine Science and Engineering Guangdong Laboratory (Zhuhai), Zhuhai, 519082, China
[2]Polar Science Center, Applied Physics Lab, University of Washington, Seattle, WA 98105, USA

Correspondence to: Hao Luo (luohao25@mail.sysu.edu.cn)

Abstract. Antarctic sea ice is an important component of the Earth system. However, its role in the Earth system is still not very clear due to limited Antarctic sea ice thickness (SIT) data. A reliable sea ice reanalysis can be useful to study Antarctic SIT and its role in the Earth system. Among various Antarctic sea ice reanalysis products, the Global Ice-Ocean Modeling and Assimilation System (GIOMAS) output is widely used in the research of Antarctic sea ice. As more Antarctic SIT observations with quality control are released, a further evaluation of Antarctic SIT from GIOMAS is conducted in this study based on in-situ and satellite observations. Generally, though only sea ice concentration is assimilated, GIOMAS can basically reproduce the observed variability of sea ice volume and its changes in the trend before and after 2013, indicating that GIOMAS is a good option to study the long-term variation of Antarctic sea ice. However, due to deficiencies in model and asymmetric changes in SIT caused by assimilation, GIOMAS underestimates Antarctic SIT especially in deformed ice regions, which has an impact on not only the mean state of SIT but also the variability. Thus, besides the further development of model, assimilating additional sea ice observations (e.g., SIT and sea ice drift) with advanced assimilation methods may be conducive to a more accurate estimation of Antarctic SIT.

1 Introduction

Antarctic sea ice plays an important role in the Earth system. Firstly, Antarctic sea ice can influence the Earth climate system. For instance, changes in Antarctic sea ice could affect freshwater flux of the Southern Ocean that directly influences the stratification of the ocean (Goosse and Zunz, 2014; Haumann et al., 2016). Besides, Antarctic sea ice acts as a protective buffer for Antarctic ice shelves, with the thinning or absence of sea ice increasing the possibility of ice shelf disintegration (Robel, 2017; Massom et al., 2018). Secondly, Antarctic sea ice has a significant impact on the biosphere of the Earth system. Studies have shown that the variation of Antarctic sea ice thickness (SIT) will affect the maximum biomass of algae in different ice layers, which will influence the food web of the Southern Ocean (Massom and Stammerjohn, 2010; Schultz, 2013). Thirdly,

Antarctic sea ice has impacts on human activities such as shipping and fishery management (Dahood et al., 2019; Mishra et al., 2021). Hence, studies on Antarctic sea ice are of great scientific and socio-economic importance.

To truly understand changes in sea ice of the Southern Ocean, SIT is needed to estimate the sea ice volume (SIV), since it is through volume changes that sea ice has its greatest impact on the water column (Maksym et al., 2012; Hobbs et al., 2016). Although changes in Antarctic sea ice extent (SIE) have been investigated extensively (Turner et al., 2015; Parkinson, 2019), they may not be a robust proxy of large scale changes in SIV, and many studies related to Antarctic sea ice are limited by the short of reliable SIT data. For example, freshwater flux of the Southern Ocean, which affects the stratification of ocean, cannot be accurately estimated (Haumann et al., 2016). In addition, the skill of sea ice prediction cannot meet the need of human activities in the Antarctic (Mishra et al., 2021). Studies have shown that the skill of Antarctic sea ice prediction could be improved with better SIT initialization (Bushuk et al., 2021). So far, Antarctic SIT data used in studies are mainly from observations, model data, and reanalysis products.

Antarctic SIT observations can be divided into in-situ and satellite observations. In-situ observations can provide the local state of Antarctic SIT. However, the brevity and sparse distribution of in-situ SIT observations pose considerable challenges to understand the large-scale characteristics of SIT (Worby et al., 2008). While satellite observations have wider spatiotemporal coverage than in-situ observations. However, previous studies indicate that there is large uncertainty in SIT data retrieval from satellite altimeters owing to the relatively small freeboard of Antarctic sea ice compared to that in the Arctic (Maksym and Markus, 2008) and the lack of knowledge about coincident snow cover thickness as well as sea ice and snow density (Alexandrov et al., 2010). In addition, results of numerical simulations are used to investigate the long-term variation of Antarctic SIT (Zhang, 2007; Holland et al., 2014), but discrepancies are identified not only between models and observations but also among models (Shu et al., 2015; Tsujino et al., 2020), indicating the large uncertainty in model estimates.

It should be noted that reanalysis has unique advantages over observed and simulated SIT. Theoretically, reanalysis can provide more accurate or comprehensive state estimations than can otherwise be obtained through either observations or models alone, which merges the information from both observations and models through data assimilation. Compared with observations, reanalysis data can provide coordinated and gridded data with homogenous sampling in time and space over a long period (Parker, 2016). And compared with model only data, reanalysis data can produce the state estimations closer to observations because of data assimilation (Lindsay and Zhang, 2006; Rollenhagen et al., 2009). Hence, SIT reanalysis data has been widely adopted in studies on the Antarctic sea ice (Abernathey et al., 2016; Kumar et al., 2017). Nevertheless, there are still large uncertainties of present sea ice reanalysis in the Southern Ocean (Uotila et al., 2019; Shi et al., 2021), suggesting the necessity and importance of evaluating them.

Among a number of Antarctic sea ice reanalysis, the Global Ice-Ocean Modeling and Assimilation System (GIOMAS) is one of the most widely used in studies of Antarctic sea ice. For instance, GIOMAS has been regarded as the reference in the assessments of simulations (Shu et al., 2015; Uotila et al., 2017; DuVivier et al., 2020) and predictions (Ordoñez et al., 2018; Morioka et al., 2021). However, GIOMAS has been less widely evaluated, in part because there are far fewer observations of Antarctic SIT against which evaluation is possible (DuVivier et al., 2020).

Due to advances in observing technology as well as algorithm in recent years, the quality of Antarctic SIT observations is improved. For example, compared to the European Remote-Sensing Satellites (i.e., ERS-1 and ERS-2), the Synthetic-Aperture

65 Interferometric Radar Altimeter (SIRAL) on board CryoSat-2 (CS2) is equipped with two radar antennas, which significantly improves the accuracy of sea ice freeboard. CS2 also has a much wider spatial coverage with improved along-track resolution because of the design of the satellite orbit and multiple operation modes (Parrinello et al., 2018). And Paul et al. (2018) developed an adaptive retracker threshold for CS2 to produce a consistent sea ice freeboard data. Besides, more Antarctic SIT observations has been available with the accumulation of observations. For instance, more in-situ observations are obtained

70 from dedicated research stations, icebreakers and autonomous underwater vehicles due to increasing research activities in the Antarctic. These provide an opportunity to further evaluate Antarctic SIT of GIOMAS.

The paper is organized as follows. In Sect. 2, Antarctic SIT from GIOMAS and observations are introduced. In Sect. 3, Antarctic SIT of GIOMAS is evaluated with observations from different aspects, including the climatology, the linear trend, the intensity of variability, as well as the frequency distribution. The final section provides the conclusions and discussion.

75 **2 Data and methods**

2.1 SIT from GIOMAS

GIOMAS consists of a global Parallel Ocean and sea Ice Model (POIM) with data assimilation capabilities, which is developed at University of Washington (Zhang and Rothrock, 2003). The ocean component of POIM is the Parallel Ocean Program, and the sea ice component of POIM is the 8-category thickness and enthalpy distribution sea ice model. The National Centres for

80 Environmental Prediction-National Centre for Atmospheric Research (NCEP-NCAR) daily reanalysis (Kalnay et al., 1996) provides the atmospheric forcing for POIM. Furthermore, in GIOMAS, the modelled sea ice concentration (SIC) is nudged towards observed SIC derived from Special Sensor Microwave Imager launched by the Defense Meteorological Satellite Program (Weaver et al., 1987), and other modelled variables including SIT are adjusted subsequently. More technical details for POIM and assimilation procedures can be found in Zhang and Rothrock (2003) and Lindsay and Zhang (2006), respectively.

85 GIOMAS data is available from 1979 to present with a global coverage and data involved in the assessment spans from January 1979 to December 2018 (Fig. 1a). The average horizontal spatial resolution is 0.8 degrees of longitude × 0.8 degrees of latitude (around 60 km × 60 km), and the temporal resolution is one month for all variables. Additionally, GIOMAS also provides daily outputs for some variables including SIT, SIC and snow depth, and the monthly SIT of GIOMAS is assessed in this study. SIT data of GIOMAS is the equivalent SIT, which represents SIV per unit area.

90 **2.2 SIT from satellite altimeters and in-situ observations**

Satellite-altimeter observations involved in this study are from radar altimeters on board Envisat (ES) and CS2, which is generated by the Sea Ice Climate Change Initiative (SICCI) project under the European Space Agency (ESA) CCI program.

ES was equipped with the Radar Altimeter 2, measuring sea ice freeboard (thickness of sea ice above sea surface) mainly based on K_u-band frequency (Hendricks et al., 2018b). The Antarctic SIT data derived from ES freeboard spans from December

95   2002 to November 2011 (Fig. 1a) with a coverage of the entire Antarctica (Fig. 1b). The spatial resolution is 50 km × 50 km and the temporal resolution is 1 month. CS2 was equipped with the SIRAL, measuring the sea ice freeboard mainly based on K_u-band frequency like ES (Hendricks et al., 2018a). CS2 Antarctic SIT dataset spans from November 2010 to April 2017 (Fig. 1a) and the spatial coverage and the spatiotemporal resolution are same as ES SIT dataset.

In-situ SIT observations involved in this study are from upward looking sonar (ULS), shipborne and airborne measurements.

100   ULS is a kind of mooring measurement at fixed locations, measuring sea ice draft (thickness of sea ice below the water surface) with a time interval shorter than 15 minutes (Behrendt et al., 2013). Ice draft needs to be converted into total SIT in an empirical way according to (Harms et al., 2001). Thirteen ULSs used in this study were deployed in the Weddell Sea (Fig. 1b) by Alfred Wegener Institute (AWI) and spanned from 1990 to 2010 intermittently (Fig. 1a).

The ship-based observations are made up of the Antarctic Sea Ice Processes & Climate program (ASPeCt), ANT-XXIX/6

105   (Schwegmann, 2013) and ANT-XXIX/7 (Ricker, 2016). The ASPeCt dataset not only includes ASPeCt observations collected from 1981 to 2005 (Worby et al., 2008), but also includes the ASPeCt bridge-based sea ice observations collected from 2007 to 2012. The ship tracks cover all sectors of the Southern Ocean (Fig. 1b) and the average spacing of data points is 6 nautical miles. The air-based SIT observations include data collected by the airborne electromagnetic system with a high frequency of 0.5 Hz and an average spacing of 3-4 m (Lemke, 2009, 2014), which is mainly located in the northwest Weddell Sea (Fig. 1b).

110   **2.3 Data processing and methods**

According to Parkinson and Cavalieri (2012), the summer, autumn, winter and spring refer to January-March, April-June, July-September and October-December, respectively. As shown in Fig. 1b, the Southern Ocean is divided into the Weddell Sea (60° W-20° E), the Indian Ocean (20° E-90°E), the western Pacific Ocean (90°E-160°E), the Ross Sea (160°E-130°W) and the Amundsen/Bellingshausen Sea (130°W-60°W).

115   All analyses in this study take place on the grid of observations, which means that GIOMAS was converted to the observed grid. Anomalies are defined as departures from the climatological annual cycle, and the intensity of variability is defined as the standard deviation of anomalies. During the overlapped time of ES and CS2 (November 2010 to November 2011), the difference in SIV anomalies between ES and CS2 (i.e., root mean squared error is 574.4 km^3) is much less than the variation of SIV anomalies (i.e., their standard deviations in ES and CS2 are 969.6 km^3 and 1004.3 km^3, respectively). Thus, ES from

120   December 2002 to October 2010 and CS2 from November 2010 to April 2017 are spliced together to calculate trend. In addition, since the trajectories of air-based SIT observations are mainly distributed in the northwest Weddell Sea where is dominated by deformed sea ice (Fig. 1b), and the amount of air-based data is much greater than that of ship-based observations due to the differences in average spacing between ship-based (i.e., 3-4 m) and air-based observations (i.e., 11 km). Therefore, the comparison between GIOMAS and air-based observations is only conducted in the Weddell Sea.

3 Results

125 Figure 2 shows the climatological annual cycle of Antarctic SIV. Although obvious uncertainties of SIV can be found in both ES and CS2, the annual cycle of ES is similar to that of CS2. Both ES and CS2 show that the melt rate of sea ice is nearly twice the growth rate. And there are also some differences in the SIV climatology between ES and CS2. The SIV of ES is greater than that of CS2 in the summer and vice versa in the winter, and larger uncertainties of SIV can be found in ES. The

130 SIV difference between ES and CS2 may be owing to differences in footprints, resolutions and retracker algorithms between the Radar Altimeter 2 on board ES and the Synthetic-Aperture Interferometric Radar Altimeter on board CS2. These differences may lead to overestimation of freeboards for ES in the first-year ice zone and overestimation of freeboards for CS2 in the multiyear ice zone and near the coasts (Schwegmann et al., 2016). GIOMAS can reproduce the asymmetry in the annual cycle of Antarctic SIV observed by ES and CS2 while underestimates SIV by about 48.5% on average when compared to ES

135 as well as CS2. And the underestimation is seasonally dependent, with weaker underestimation in summer and stronger one in winter.

Figure 3 shows the spatial distribution of SIT bias in summer as well as winter to investigate details of SIV underestimation in these two seasons. In both seasons, significant negative SIT bias of GIOMAS can be found in the deformed ice zone, such as the northwestern Weddell Sea and coasts of the Amundsen/Bellingshausen Sea as well as the East Antarctic. While the

140 extent of negative bias is wider in the winter (Figs. 3b and d) rather than in the summer (Figs. 3a and c), which results in seasonal differences of the SIV underestimation (Fig. 2). In addition, there are weakly positive SIT biases in the southwestern Weddell Sea during winter (Figs. 3b and d), which may be due to model bias in simulating sea ice transport in the western Weddell Sea (Shi et al., 2021). Considering sea ice deformation is also related to sea ice motion tightly, a better simulation of sea ice motion is required to achieve more accurate reconstruction of Antarctic SIT. And the positive bias in winter Ross Sea

145 SIT can only be found in the comparison between GIOMAS and CS2, maybe caused by smaller freeboard of CS2 than ES in the winter Weddell Sea (Schwegmann et al., 2016). Notably, it is still disputed whether radar altimeter signals originate from the snow/ice or snow/air interface or from somewhere in-between. These uncertainties, combined with often thick snow and complex snow metamorphism in the Antarctic, may contribute to the overestimation of the Antarctic SIT from ES and CS2. Thus, the underestimation of SIT from GIOMAS may be partially attributed to the uncertainties of SIT retrieved from ES and

150 CS2.

Due to large uncertainties in above satellite observations, the SIT of GIOMAS is further assessed by ULS measurement in the Weddell Sea. Considering significant variation of sea ice over horizontal distances as small as a few meters, the standard deviation of ULS is displayed in Fig. 4a. It is obvious that the variability of ULS near the shore (e.g., 206, 207, 212, 217, 232 and 233) is stronger than that of ULS far from the shore (e.g., 208, 209, 210, 227, 229, 230 and 231), indicating larger sea ice

155 deformation near the shore. As Fig. 4b shows, GIOMAS significantly underestimates the nearshore SIT all year round while slightly overestimates SIT far from shore in the winter, implying the deficiency of GIOMAS in the simulation of sea ice deformation, which leads to underestimation of SIT in the Weddell Sea from a perspective of regional average. The above

deficiency of GIOMAS might be attributed to the insufficient model resolution, which is not able to well resolve the coastal lines and hinders GIOMAS from reproducing the ice deformation near shore. Therefore, GIOMAS is indeed to underestimate
160   the climatology of Antarctic SIT, mainly in the deformed sea ice zone, compared with satellite and in-situ observations. In addition to the model drawbacks of GIOMAS, this underestimation might also be introduced by the assimilation procedure of GIOMAS. Although only satellite SIC is nudged in GIOMAS, it will modify the SIT distribution to accommodate the change in SIC, which removes sea ice from the distribution without considering its SIT if modelled SIC is too large, while adds sea ice to the 0.1-m ice thickness bin if modelled SIC is too small. This asymmetric addition and removal of ice leads to a thinning
165   of the mean ice thickness (Lindsay and Zhang, 2006).

Antarctic SIE shows different trends before and after 2014 (Parkinson, 2019), and SIV can better represent the overall sea ice state. Therefore, it is necessary to examine whether there are similar changes in the trend of Antarctic SIV. As Figure 5 shows, the observed Antarctic SIV anomaly increased gradually from 2003, reached the maximum (3158.1 km^3) in November 2013, and then abruptly declined from September 2013 to April 2017. The evolution of SIV anomaly is comparable to that of SIE
170   anomaly, while the time of the SIV anomaly peak is earlier than that of the SIE anomaly peak nearly by one year. Although there are differences in the SIV trend between GIOMAS and satellite observation, GIOMAS can basically reproduce the changes in the observed SIV trend before and after 2013. Besides, the correlation of SIV anomalies between GIOMAS and observations is 0.82, which passes a two-tailed t test at 99% significant level. And given the advantages of reanalysis over observations or models individually especially in the polar region (Buehner et al., 2017), GIOMAS data would be a good
175   choice to study the variability and long-term trends of Antarctic sea ice.

Considering the obvious variability of SIV in Fig. 5, Figure 6 displays spatial differences in the intensity of SIT anomalies variability between GIOMAS and satellite observations. Compared with ES and CS2, GIOMAS underestimates the SIT variability in the Southern Ocean, especially in the deformed ice zone (Figs. 6a-b), which resembles the spatial pattern of Fig. 3. The underestimation can be found also in the comparison between GIOMAS and ULS. The SIT variability is underestimated
180   near the shore, while overestimated away from the shore (Fig. 6c), which is consistent with Fig. 4b. These phenomena suggest that there appears to be a relationship between the mean SIT and the variability. As Blanchard-Wrigglesworth and Bitz (2014) suggested, models with a thinner mean ice state tend to have SIT anomalies with smaller amplitude. Thus, the bias of SIT has an impact not only on the climatology of SIT but also on the variability of SIT.

In addition to ULS observations, the rest of in-situ sea ice observations is sparse in the Southern Ocean and mainly provided
185   by shipborne and airborne measurements. Figure 7 shows the SIT frequency distribution of GIOMAS and ship-based as well as air-based in-situ observations. The peaks of observations are mainly around 0-0.6 m while the frequencies of GIOMAS SIT are mainly distributed in 0-1.4 m in the Southern Ocean (Fig. 7a). In different sectors (Figs. 7b-f), the frequency distribution of observed SIT data is similar to that in the whole Southern Ocean while the peak of GIOMAS SIT frequency varies from 0.2 m to 1.4 m. Compared with observations, for the Southern Ocean, GIOMAS has a higher frequency within 0.6-1.8 m while a
190   lower frequency in the rest bins compared with ship-based observations (Fig. 7a), which seems to imply the overestimation of SIT. And similar results can be found in different sectors (Figs. 7b-f). However, the sample selection bias should be noted in

the ship-based observations due to ship's track avoiding areas of thicker ice, which results in its estimation biased toward thinner ice (Timmermann, 2004; Williams et al., 2015). Besides, GIOMAS has a lower frequency of thick ice in the Weddell Sea compared with air-based observations, suggesting the weakness of GIOMAS in the simulation of sea ice deformation.

195 **4 Conclusions and discussion**

Considering the important role of SIT in studies of Antarctic sea ice and the wide application of GIOMAS, the Antarctic SIT of GIOMAS is assessed in this paper with satellite and in-situ observations. In general, GIOMAS can basically reproduce the observed variability and linear trends of SIV even though only satellite SIC data is assimilated by nudging. For the climatology, GIOMAS can reproduce the asymmetry in the annual cycle of Antarctic SIV. For the long-term SIV variation, the variation of

200 GIOMAS is in phase with that of observations, and it is also able to capture the changes in linear trends before and after 2013. These suggest that GIOMAS is useful to study the long-term variation of Antarctic sea ice. However, significant negative bias in SIT can be found in the comparison between of GIOMAS and observations. Compared with satellite measurements, GIOMAS tends to underestimate SIT, especially in regions of strong ice deformation. And this underestimation is of seasonal dependence with greater underestimation in the winter. Although above underestimation can be partially attributed to the

205 uncertainties of SIT retrieved from satellite, SIT underestimation in the northwest Weddell Sea is further verified by the comparison between GIOMAS and ULS observations. And the spatial distribution of the differences in the magnitude of SIT variability resembles that of the differences in SIT climatology between GIOMAS and observations. And given the relationship between mean state of SIT and variability (Blanchard-Wrigglesworth and Bitz, 2014), this phenomenon indicates that SIT underestimation might have an impact on not only the SIT climatology but also the SIT variability. In addition, GIOMAS

210 underestimates SIT in the Weddell Sea compared with air-baased observations while overestimates SIT compared with ship-based observations, which can be due to the negative bias in ship-based SIT estimation (Timmermann, 2004; Williams et al., 2015).

However, this study is also limited by observations of Antarctic SIT due to their unsuitability for the evaluation. For example, though SIT from ICESat (Kern et al., 2016) equipped with the Geoscience Laser Altimeter System is available from 2004 to

215 2008 and proved to have lower bias in SIT estimation than radar altimeter measurements (Willatt et al., 2010; Wang et al., 2020), it is not adopted in this study. The reasons are as follows. First, ICESat SIT is not available in winter (July-September), when greater underestimation of SIT is found in GIOMAS (Fig. 2). Second, the data size of ICESat is relatively smaller than that of ES and CS2 because ICESat provides seasonal mean data and its time range is narrower. Therefore, the additional assessment on SIT of GIOMAS will be conducted when the Antarctic SIT derived from ICESat-2 is available.

220 The above SIT underestimation of GIOMAS can be partially attributed to the model weakness. For example, insufficient model resolution restricts GIOMAS to reproduce the ice deformation near shore. And also the asymmetric SIT changes introduced by assimilation cannot be ignored in GIOMAS. Thus, besides the further development of the model, there are two suggested ways to improve the estimation of Antarctic SIT from the perspective of data assimilation. Firstly, additional sea ice

observations other than SIC should be assimilated. For example, besides Antarctic SIT derived from EnviSat-2 and CryoSat-

225 2 used in this study, the Antarctic SIT retrieved from ICESat-2 is also to be released in the near future, and hence assimilating these SIT observations directly may suppress the bias of SIT (e.g., Yang et al., 2014; Fritzner et al., 2019; Luo et al., 2021). Also, assimilating sea ice drift observations can improve the simulation of sea ice motion and deformation, which can improve the estimation of SIT (e.g., Lindsay and Zhang, 2006; Mu et al., 2020). Secondly, advanced data assimilation methods should be adopted to provide balanced estimation of model state. For instance, the innovation of SIC can be converted to the increment

230 of SIT in a more balanced way through the flow-dependent covariance of Ensemble Kalman Filter (e.g., Massonnet et al., 2013; Yang et al., 2015).

Besides, in the course of global warming, Antarctic SIE rose gradually and reached a record high in 2014 before decreasing dramatically, which is obviously different from the dramatic drop in Arctic SIE during the satellite era (e.g., Turner and Comiso, 2017). Results from a recent study suggest that the trend in Antarctic ice coverage may be due to changes in atmospheric (e.g.,

235 Holland and Kwok, 2012) and oceanic (e.g., Meehl et al., 2019) processes. Without better SIT and SIV estimates, it is difficult to characterize how Antarctic sea ice cover is responding to changing climate, or which climate parameters are most influential (Vaughan et al., 2013). Thus, more Antarctic sea ice observations and more studies on data assimilation are urgently needed to accurately evaluate the Antarctic SIT, which can help to improve the reconstruction and prediction of Antarctic SIV and to support research related to Antarctic sea ice.

240 **Data availability**

The GIOMAS reanalysis data are available at http://psc.apl.washington.edu/zhang/Global_seaice/data.html. The satellite-based Antarctic sea ice thickness observations from Envisat and CryoSat-2 are available at https://doi.org/10.5285/b1f1ac03077b4aa784c5a413a2210bf5 and https://doi.org/10.5285/48fc3d1e8ada405c8486ada522dae9e8, respectively. The Weddell Sea upward-looking sonar sea ice

245 draft data are available at https://doi.pangaea.de/10.1594/PANGAEA.785565. The shipborne sea ice thickness observations are available at http://aspect.antarctica.gov.au/data, https://doi.org/10.1594/PANGAEA.819540 and https://doi.org/10.1594/PANGAEA.831976. The sea ice thickness observations from airborne electromagnetic system are freely available at https://doi.pangaea.de/10.1594/PANGAEA.771229 and https://epic.awi.de/id/eprint/36245/.

Author contribution

250 QY and HL developed the concept of the paper. SL and HL performed analysis and drafted the manuscript. JW collected the remote sensing and observation data. QY, JZ, QS and JW gave comments and helped revise the manuscript. All of the co-authors contributed to scientific interpretations.

Competing interests

The authors declare that they have no conflict of interest.

255 **Acknowledgments**

This study is supported by the National Natural Science Foundation of China (No. 41941009, 41922044, 42006191), and the Guangdong Basic and Applied Basic Research Foundation (No. 2020B1515020025). This is a contribution to the Year of Polar Prediction (YOPP), a flagship activity of the Polar Prediction Project (PPP), initiated by the World Weather Research Programme (WWRP) of the World Meteorological Organisation (WMO). We acknowledge the WMO WWRP for its role in
260 coordinating this international research activity.

References

Abernathey, R. P., Cerovecki, I., Holland, P. R., Newsom, E., Mazloff, M., and Talley, L. D.: Water-mass transformation by sea ice in the upper branch of the Southern Ocean overturning, Nat. Geosci., 9, 596-601, https://doi.org/10.1038/ngeo2749, 2016.

265 Alexandrov, V., Sandven, S., Wahlin, J., and Johannessen, O. M.: The relation between sea ice thickness and freeboard in the Arctic, The Cryosphere, 4, 373-380, https://doi.org/10.5194/tc-4-373-2010, 2010.

Behrendt, A., Dierking, W., Fahrbach, E., and Witte, H.: Sea ice draft in the Weddell Sea, measured by upward looking sonars, Earth Syst. Sci. Data, 5, 209-226, https://doi.org/10.5194/essd-5-209-2013, 2013.

Blanchard-Wrigglesworth, E., and Bitz, C. M.: Characteristics of Arctic Sea-Ice Thickness Variability in GCMs, J. Climate,
270 27, 8244-8258, https://doi.org/10.1175/jcli-d-14-00345.1, 2014.

Buehner, M., Bertino, L., Caya, A., Heimbach, P., and Smith, G.: Sea Ice Data Assimilation, in: Sea Ice Analysis and Forecasting: Towards an Increased Reliance on Automated Prediction Systems, edited by: Lemieux, J.-F., Toudal Pedersen, L., Buehner, M., and Carrieres, T., Cambridge University Press, Cambridge, 51-108, https://doi.org/10.1017/9781108277600.005, 2017.

275 Bushuk, M., Winton, M., Haumann, F. A., Delworth, T., Lu, F., Zhang, Y., Jia, L., Zhang, L., Cooke, W., Harrison, M., Hurlin, B., Johnson, N. C., Kapnick, S., McHugh, C., Murakami, H., Rosati, A., Tseng, K.-C., Wittenberg, A. T., Yang, X., and Zeng, F.: Seasonal prediction and predictability of regional Antarctic sea ice, J. Climate, 1-68, https://doi.org/10.1175/jcli-d-20-0965.1, 2021.

Dahood, A., Watters, G. M., and de Mutsert, K.: Using sea-ice to calibrate a dynamic trophic model for the Western Antarctic
280 Peninsula, PloS One, 14, e0214814, https://doi.org/10.1371/journal.pone.0214814, 2019.

DuVivier, A. K., Holland, M. M., Kay, J. E., Tilmes, S., Gettelman, A., and Bailey, D. A.: Arctic and Antarctic Sea Ice Mean State in the Community Earth System Model Version 2 and the Influence of Atmospheric Chemistry, J. Geophys. Res.-Oceans, 125, e2019JC015934, https://doi.org/10.1029/2019JC015934, 2020.

Fritzner, S., Graversen, R., Christensen, K. H., Rostosky, P., and Wang, K.: Impact of assimilating sea ice concentration, sea
285 ice thickness and snow depth in a coupled ocean–sea ice modelling system, The Cryosphere, 13, 491-509, https://doi.org/10.5194/tc-13-491-2019, 2019.

Goosse, H., and Zunz, V.: Decadal trends in the Antarctic sea ice extent ultimately controlled by ice–ocean feedback, The Cryosphere, 8, 453-470, https://doi.org/10.5194/tc-8-453-2014, 2014.

Harms, S., Fahrbach, E., and Strass, V. H.: Sea ice transports in the Weddell Sea, Journal of Geophysical Research-Oceans,
290 106, 9057-9073, https://doi.org/10.1029/1999jc000027, 2001.

Haumann, F. A., Gruber, N., Münnich, M., Frenger, I., and Kern, S.: Sea-ice transport driving Southern Ocean salinity and its recent trends, Nature, 537, 89-92, https://doi.org/10.1038/nature19101, 2016.

Hendricks, S., Paul, S., and Rinne, E.: ESA Sea Ice Climate Change Initiative (Sea_Ice_cci): Southern hemisphere sea ice thickness from the CryoSat-2 satellite on a monthly grid (L3C), v2.0, Centre for Environmental Data Analysis,
295 https://doi.org/10.5285/48fc3d1e8ada405c8486ada522dae9e8, 2018a.

Hendricks, S., Paul, S., and Rinne, E.: ESA Sea Ice Climate Change Initiative (Sea_Ice_cci): Southern hemisphere sea ice thickness from the Envisat satellite on a monthly grid (L3C), v2.0, https://doi.org/10.5285/b1f1ac03077b4aa784c5a413a2210bf5, 2018b.

Hobbs, W. R., Massom, R., Stammerjohn, S., Reid, P., Williams, G., and Meier, W.: A review of recent changes in Southern
300 Ocean sea ice, their drivers and forcings, Global Planet. Change, 143, 228-250, https://doi.org/10.1016/j.gloplacha.2016.06.008, 2016.

Holland, P. R., and Kwok, R.: Wind-driven trends in Antarctic sea-ice drift, Nat. Geosci., 5, 872-875, https://doi.org/10.1038/ngeo1627, 2012.

Holland, P. R., Bruneau, N., Enright, C., Losch, M., Kurtz, N. T., and Kwok, R.: Modeled Trends in Antarctic Sea Ice
305 Thickness, J. Climate, 27, 3784-3801, https://doi.org/10.1175/jcli-d-13-00301.1, 2014.

Kalnay, E., Kanamitsu, M., Kistler, R., Collins, W., Deaven, D., Gandin, L., Iredell, M., Saha, S., White, G., Woollen, J., Zhu, Y., Chelliah, M., Ebisuzaki, W., Higgins, W., Janowiak, J., Mo, K. C., Ropelewski, C., Wang, J., Leetmaa, A., Reynolds, R., Jenne, R., and Joseph, D.: The NCEP/NCAR 40-year reanalysis project, B. Am. Meteorol. Soc., 77, 437-471, https://doi.org/10.1175/1520-0477(1996)077<0437:tnyrp>2.0.co;2, 1996.

310 Kern, S., Ozsoy-Çiçek, B., and Worby, A.: Antarctic Sea-Ice Thickness Retrieval from ICESat: Inter-Comparison of Different Approaches, Remote Sens.-Basel, 8, https://doi.org/10.3390/rs8070538, 2016.

Kumar, A., Dwivedi, S., and Rajak, D. R.: Ocean sea-ice modelling in the Southern Ocean around Indian Antarctic stations, Journal of Earth System Science, 126, 70, https://doi.org/10.1007/s12040-017-0848-5, 2017.

Lemke, P.: The Expedition of the Research Vessel Polarstern to the Antarctic in 2006 (ANT-XXIII/7), Alfred-Wegener-Institut

315   für Polar- und Meeresforschung;, Bremerhaven, Germany1866-3192, 1-147, 2009.

Lemke, P.: The Expedition of the Research Vessel Polarstern to the Antarctic in 2013 (ANT-XXIX/6), Alfred-Wegener-Institut, Helmholtz-Zentrum für Polar- und Meeresforschung;, Bremerhaven, Germany1866-3192, 1-154, 2014.

Lindsay, R. W., and Zhang, J.: Assimilation of ice concentration in an ice–ocean model, J. Atmos. Ocean. Tech., 23, 742-749, https://doi.org/10.1175/jtech1871.1, 2006.

320   Luo, H., Yang, Q., Mu, L., Tian-Kunze, X., Nerger, L., Mazloff, M., Kaleschke, L., and Chen, D.: DASSO: a data assimilation system for the Southern Ocean that utilizes both sea-ice concentration and thickness observations, J. Glaciol., 1-6, https://doi.org/10.1017/jog.2021.57, 2021.

Maksym, T., and Markus, T.: Antarctic sea ice thickness and snow-to-ice conversion from atmospheric reanalysis and passive microwave snow depth, J. Geophys. Res., 113, https://doi.org/10.1029/2006jc004085, 2008.

325   Maksym, T., Stammerjohn, S., Ackley, S., and Massom, R.: Antarctic Sea Ice—A Polar Opposite?, Oceanography, 25, 140-151, https://doi.org/10.5670/oceanog.2012.88, 2012.

Massom, R. A., and Stammerjohn, S. E.: Antarctic sea ice change and variability – Physical and ecological implications, Polar Sci., 4, 149-186, https://doi.org/10.1016/j.polar.2010.05.001, 2010.

Massom, R. A., Scambos, T. A., Bennetts, L. G., Reid, P., Squire, V. A., and Stammerjohn, S. E.: Antarctic ice shelf

330   disintegration triggered by sea ice loss and ocean swell, Nature, 558, 383-389, https://doi.org/10.1038/s41586-018-0212-1, 2018.

Massonnet, F., Mathiot, P., Fichefet, T., Goosse, H., Beatty, C. K., Vancoppenolle, M., and Lavergne, T.: A model reconstruction of the Antarctic sea ice thickness and volume changes over 1980-2008 using data assimilation, Ocean Model., 64, 67-75, https://doi.org/10.1016/j.ocemod.2013.01.003, 2013.

335   Meehl, G. A., Arblaster, J. M., Chung, C. T. Y., Holland, M. M., DuVivier, A., Thompson, L., Yang, D., and Bitz, C. M.: Sustained ocean changes contributed to sudden Antarctic sea ice retreat in late 2016, Nat. Commun., 10, 14, https://doi.org/10.1038/s41467-018-07865-9, 2019.

Mishra, P., Alok, S., Rajak, D. R., Beg, J. M., Bahuguna, I. M., and Talati, I.: Investigating optimum ship route in the Antarctic in presence of sea ice and wind resistances – A case study between Bharati and Maitri, Polar Sci.,

340   https://doi.org/10.1016/j.polar.2021.100696, 2021.

Morioka, Y., Iovino, D., Cipollone, A., Masina, S., and Behera, S. K.: Summertime sea-ice prediction in the Weddell Sea improved by sea-ice thickness initialization, Sci. Rep.-UK, 11, 11475, https://doi.org/10.1038/s41598-021-91042-4, 2021.

Mu, L., Nerger, L., Tang, Q., Loza, S. N., Sidorenko, D., Wang, Q., Semmler, T., Zampieri, L., Losch, M., and Goessling, H. F.: Toward a data assimilation system for seamless sea ice prediction based on the AWI climate model, J. Adv. Model. Earth.

345   Sy., 12, e2019MS001937, https://doi.org/10.1029/2019ms001937, 2020.

Ordoñez, A. C., Bitz, C. M., and Blanchard-Wrigglesworth, E.: Processes controlling Arctic and Antarctic sea ice predictability in the Community Earth System Model, J. Climate, 31, 9771-9786, https://doi.org/10.1175/jcli-d-18-0348.1, 2018.

Parker, W. S.: Reanalyses and observations: What's the difference?, B. Am. Meteorol. Soc., 97, 1565-1572, https://doi.org/10.1175/bams-d-14-00226.1, 2016.

350 Parkinson, C. L., and Cavalieri, D. J.: Antarctic sea ice variability and trends, 1979–2010, The Cryosphere, 6, 871-880, https://doi.org/10.5194/tc-6-871-2012, 2012.

Parkinson, C. L.: A 40-y record reveals gradual Antarctic sea ice increases followed by decreases at rates far exceeding the rates seen in the Arctic, P. Natl. Acad. Sci. USA, 116, 14414-14423, https://doi.org/10.1073/pnas.1906556116, 2019.

Parrinello, T., Shepherd, A., Bouffard, J., Badessi, S., Casal, T., Davidson, M., Fornari, M., Maestroni, E., and Scagliola, M.:
355 CryoSat: ESA's ice mission – Eight years in space, Advances in Space Research, 62, 1178-1190, https://doi.org/10.1016/j.asr.2018.04.014, 2018.

Paul, S., Hendricks, S., Ricker, R., Kern, S., and Rinne, E.: Empirical parametrization of Envisat freeboard retrieval of Arctic and Antarctic sea ice based on CryoSat-2: progress in the ESA Climate Change Initiative, The Cryosphere, 12, 2437-2460, https://doi.org/10.5194/tc-12-2437-2018, 2018.

360 Ricker, R.: Sea ice conditions during POLARSTERN cruise ANT-XXIX/7, PANGAEA, https://doi.org/10.1594/PANGAEA.831976, 2016.

Robel, A. A.: Thinning sea ice weakens buttressing force of iceberg mélange and promotes calving, Nat. Commun., 8, 14596, https://doi.org/10.1038/ncomms14596, 2017.

Rollenhagen, K., Timmermann, R., Janjić, T., Schröter, J., and Danilov, S.: Assimilation of sea ice motion in a finite-element
365 sea ice model, J. Geophys. Res., 114, https://doi.org/10.1029/2008jc005067, 2009.

Schultz, C.: Antarctic sea ice thickness affects algae populations, Eos, Transactions American Geophysical Union, 94, 40-40, https://doi.org/10.1002/2013EO030032, 2013.

Schwegmann, S.: Sea ice conditions during POLARSTERN cruise ANT-XXIX/6 (AWECS), PANGAEA, https://doi.org/10.1594/PANGAEA.819540, 2013.

370 Schwegmann, S., Rinne, E., Ricker, R., Hendricks, S., and Helm, V.: About the consistency between Envisat and CryoSat-2 radar freeboard retrieval over Antarctic sea ice, The Cryosphere, 10, 1415-1425, https://doi.org/10.5194/tc-10-1415-2016, 2016.

Shi, Q., Yang, Q., Mu, L., Wang, J., Massonnet, F., and Mazloff, M. R.: Evaluation of sea-ice thickness from four reanalyses in the Antarctic Weddell Sea, The Cryosphere, 15, 31-47, https://doi.org/10.5194/tc-15-31-2021, 2021.

375 Shu, Q., Song, Z.-Y., and Qiao, F.-L.: Assessment of sea ice simulations in the CMIP5 models, The Cryosphere, 9, 399-409, https://doi.org/10.5194/tc-9-399-2015, 2015.

Timmermann, R.: Utilizing the ASPeCt sea ice thickness data set to evaluate a global coupled sea ice–ocean model, J. Geophys. Res., 109, https://doi.org/10.1029/2003jc002242, 2004.

Tsujino, H., Urakawa, L. S., Griffies, S. M., Danabasoglu, G., Adcroft, A. J., Amaral, A. E., Arsouze, T., Bentsen, M.,
380 Bernardello, R., Böning, C. W., Bozec, A., Chassignet, E. P., Danilov, S., Dussin, R., Exarchou, E., Fogli, P. G., Fox-Kemper, B., Guo, C., Ilicak, M., Iovino, D., Kim, W. M., Koldunov, N., Lapin, V., Li, Y., Lin, P., Lindsay, K., Liu, H., Long, M. C.,

Komuro, Y., Marsland, S. J., Masina, S., Nummelin, A., Rieck, J. K., Ruprich-Robert, Y., Scheinert, M., Sicardi, V., Sidorenko, D., Suzuki, T., Tatebe, H., Wang, Q., Yeager, S. G., and Yu, Z.: Evaluation of global ocean–sea-ice model simulations based on the experimental protocols of the Ocean Model Intercomparison Project phase 2 (OMIP-2), Geosci. Model Dev., 13, 3643-3708, https://doi.org/10.5194/gmd-13-3643-2020, 2020.

Turner, J., Hosking, J. S., Bracegirdle, T. J., Marshall, G. J., and Phillips, T.: Recent changes in Antarctic Sea Ice, Philos. T. R. Soc. A., 373, https://doi.org/10.1098/rsta.2014.0163, 2015.

Turner, J., and Comiso, J.: Solve Antarctica's sea-ice puzzle, Nature, 547, 275-277, https://doi.org/10.1038/547275a, 2017.

Uotila, P., Iovino, D., Vancoppenolle, M., Lensu, M., and Rousset, C.: Comparing sea ice, hydrography and circulation between NEMO3.6 LIM3 and LIM2, Geosci. Model Dev., 10, 1009-1031, https://doi.org/10.5194/gmd-10-1009-2017, 2017.

Uotila, P., Goosse, H., Haines, K., Chevallier, M., Barthélemy, A., Bricaud, C., Carton, J., Fučkar, N., Garric, G., Iovino, D., Kauker, F., Korhonen, M., Lien, V. S., Marnela, M., Massonnet, F., Mignac, D., Peterson, K. A., Sadikni, R., Shi, L., Tietsche, S., Toyoda, T., Xie, J., and Zhang, Z.: An assessment of ten ocean reanalyses in the polar regions, Clim. Dyn., 52, 1613-1650, https://doi.org/10.1007/s00382-018-4242-z, 2019.

Vaughan, D. G., Comiso, J. C., Allison, I., Carrasco, J., Kaser, G., Kwok, R., Mote, P., Murray, T., Paul, F., Ren, J.-W., E. Rignot, E., Solomina, O., Steffen, K., and Zhang, T.-J.: Observations: Cryosphere, in: Climate change 2013: The physical science basis. Contribution of working group I to the fifth assessment report of the intergovernmental panel on climate change, edited by: Stocker, T. F., Qin, D.-H., Plattner, G.-K., Tignor, M., Allen, S. K., Boschung, J., Nauels, A., Xia, Y., Bex, V., and Midgley, P. M., Cambridge University Press, Cambridge, United Kingdom and New York, NY, USA, 317-382, https://doi.org/10.1017/CBO9781107415324.012, 2013.

Wang, J., Min, C., Ricker, R., Yang, Q., Shi, Q., Han, B., and Hendricks, S.: A comparison between Envisat and ICESat sea ice thickness in the Antarctic, The Cryosphere Discuss., 2020, 1-26, https://doi.org/10.5194/tc-2020-48, 2020.

Weaver, R., Morris, C., and Barry, R. G.: Passive microwave data for snow and ice research: Planned products from the DMSP SSM/I System, Eos, Transactions American Geophysical Union, 68, 769-777, https://doi.org/10.1029/EO068i039p00769, 1987.

Willatt, R. C., Giles, K. A., Laxon, S. W., Stone-Drake, L., and Worby, A. P.: Field Investigations of Ku-Band Radar Penetration Into Snow Cover on Antarctic Sea Ice, IEEE Transactions on Geoscience and Remote Sensing, 48, 365-372, https://doi.org/10.1109/TGRS.2009.2028237, 2010.

Williams, G., Maksym, T., Wilkinson, J., Kunz, C., Murphy, C., Kimball, P., and Singh, H.: Thick and deformed Antarctic sea ice mapped with autonomous underwater vehicles, Nat. Geosci., 8, 61-67, https://doi.org/10.1038/ngeo2299, 2015.

Worby, A. P., Geiger, C. A., Paget, M. J., Van Woert, M. L., Ackley, S. F., and DeLiberty, T. L.: Thickness distribution of Antarctic sea ice, J. Geophys. Res.-Oceans, 113, https://doi.org/10.1029/2007JC004254, 2008.

Yang, Q., Losa, S. N., Losch, M., Tian-Kunze, X., Nerger, L., Liu, J., Kaleschke, L., and Zhang, Z.: Assimilating SMOS sea ice thickness into a coupled ice-ocean model using a local SEIK filter, J. Geophys. Res.-Oceans, 119, 6680-6692, https://doi.org/10.1002/2014jc009963, 2014.

Yang, Q., Losa, S. N., Losch, M., Liu, J., Zhang, Z., Nerger, L., and Yang, H.: Assimilating summer sea-ice concentration into a coupled ice-ocean model using a LSEIK filter, Ann Glaciol., 56, 38-44, https://doi.org/10.3189/2015AoG69A740, 2015.

Zhang, J., and Rothrock, D. A.: Modeling global sea ice with a thickness and enthalpy distribution model in generalized curvilinear coordinates, Mon. Weather Rev., 131, 845-861, https://doi.org/10.1175/1520-0493(2003)131<0845:Mgsiwa>2.0.Co;2, 2003.

420

Zhang, J.: Increasing Antarctic Sea Ice under Warming Atmospheric and Oceanic Conditions, J. Climate, 20, 2515-2529, https://doi.org/10.1175/jcli4136.1, 2007.

424
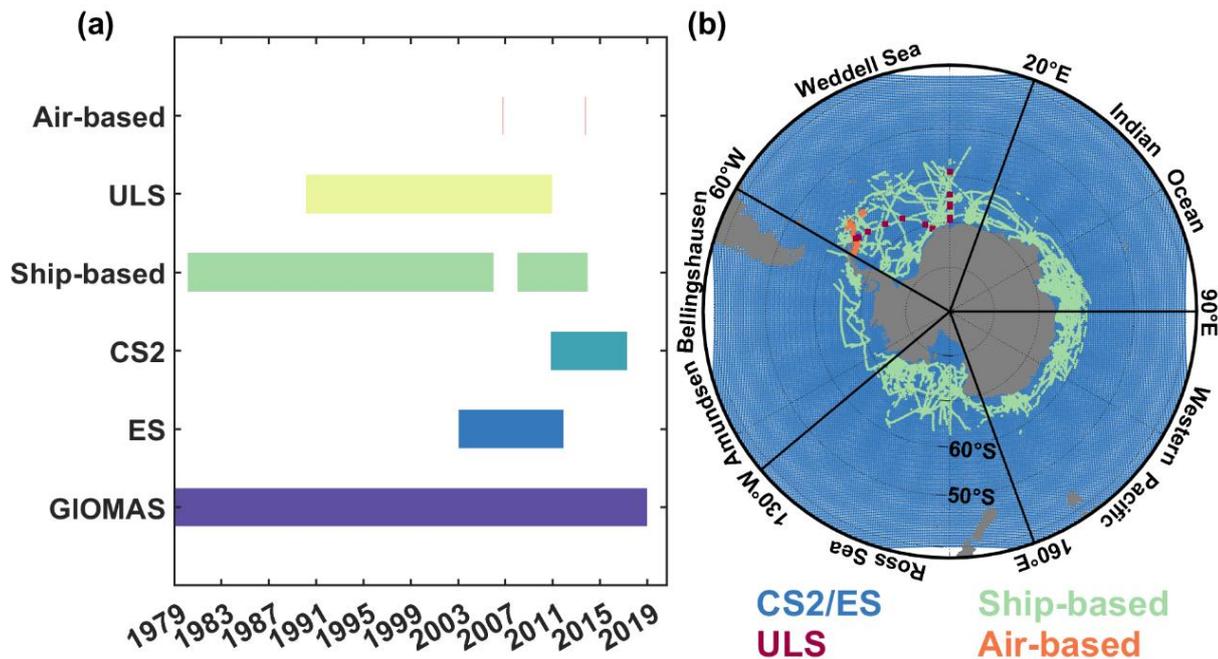
425
426   **Figure 1: (a) The temporal and (b) spatial coverage of data used in this study.**

427
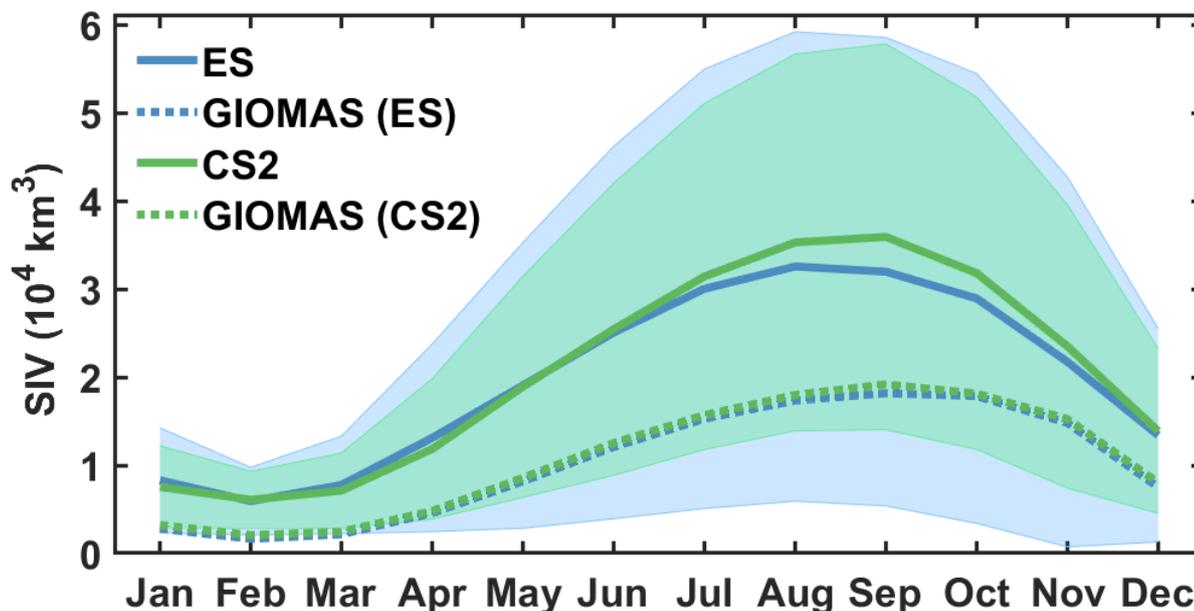
Figure 2: The climatological annual cycle of Antarctic SIV. The blue and green denote data related to ES and CS2, respectively. The solid and dashed curves denote satellite observations and corresponding GIOMAS data. The shading denotes the SIV uncertainty of satellite observations.
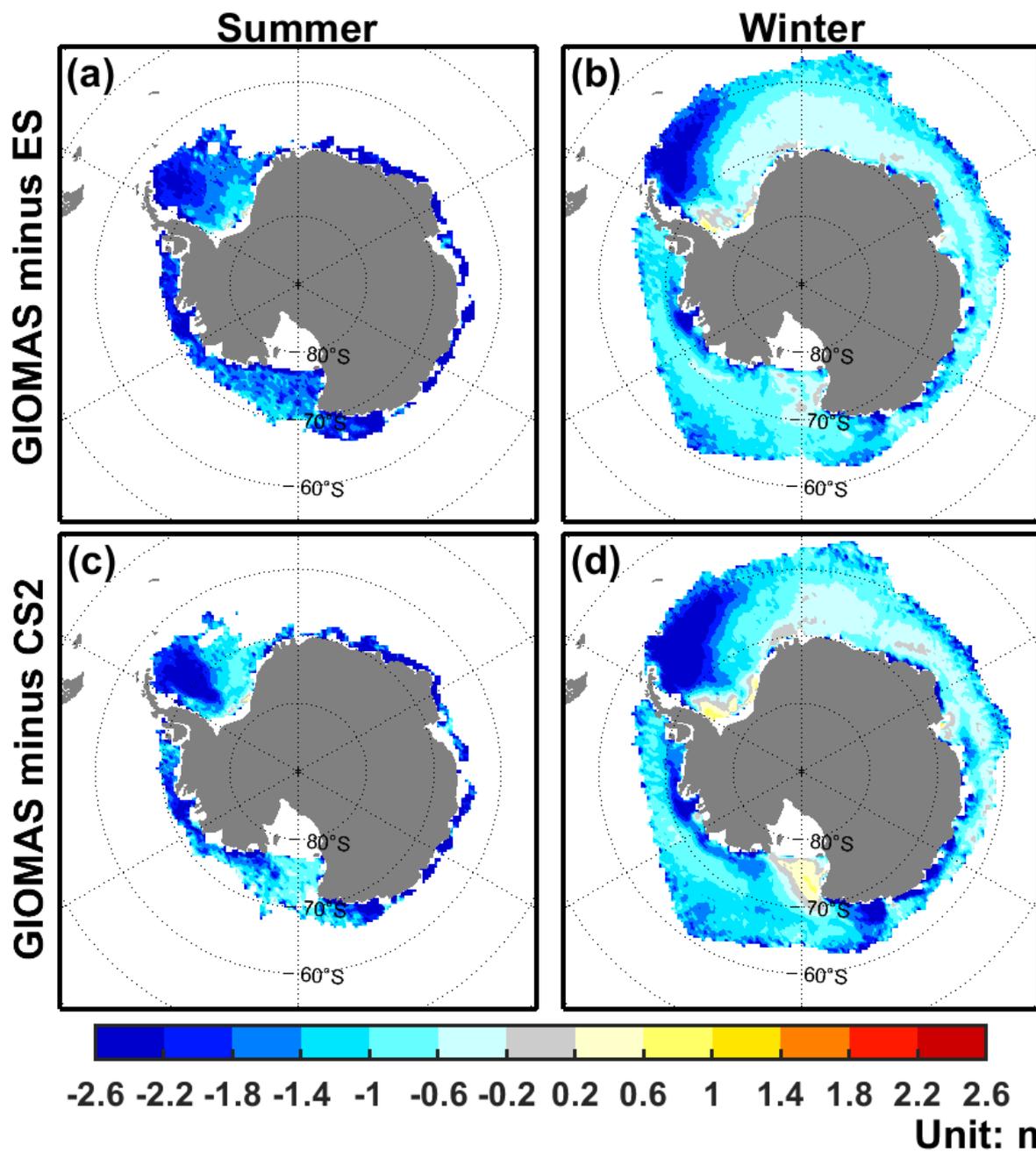
Figure 3: The SIT bias of GIOMAS relative to ES in (a) the summer and (b) winter. (c-d) same as (a-b) but for bias relative to CS2.
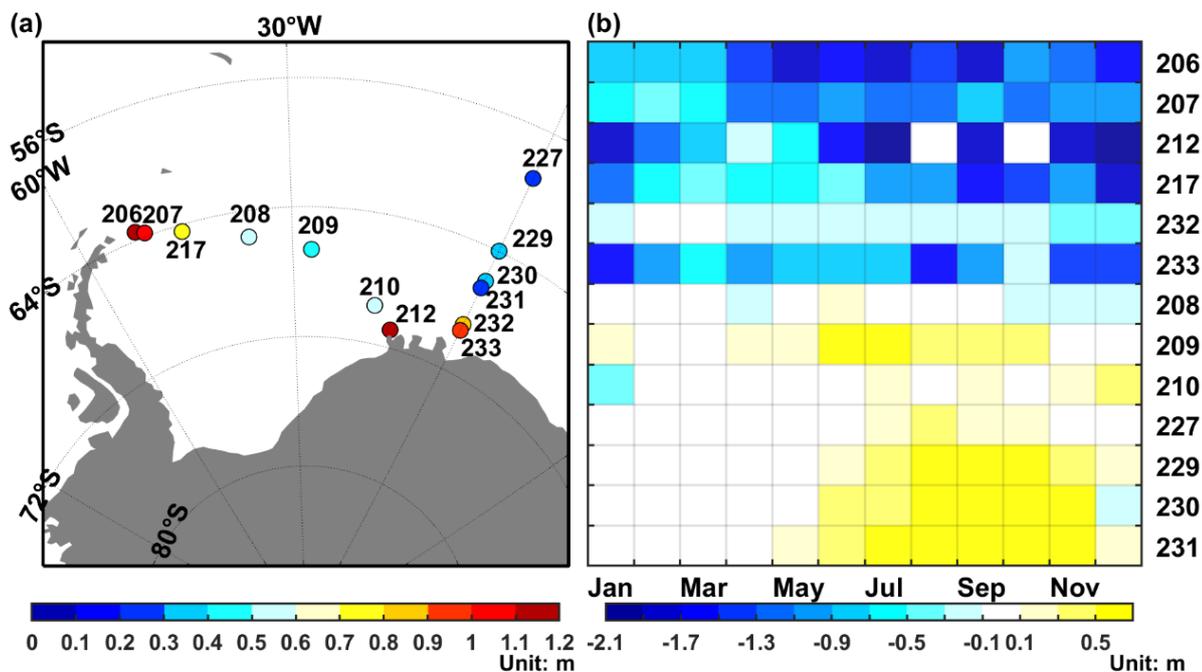
Figure 4: (a) The locations of ULS in the Weddell Sea and corresponding standard deviation of SIT. (b) The differences in SIT climatology between GIOMAS and ULS.
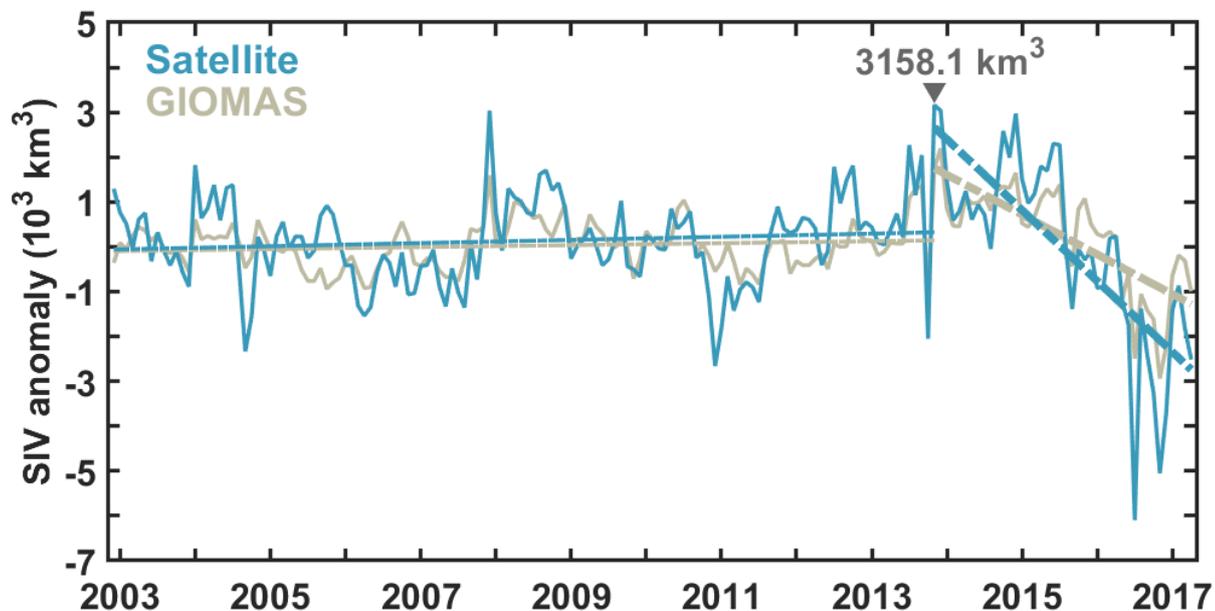
440
441 **Figure 5: The SIV anomalies of satellite observations (green) and corresponding GIOMAS (khaki). The satellite observations used**
442 **here are made up with ES and CS2 together as descripted in Sect. 2.3. Dashed lines denote the linear trends of SIV anomalies**
443 **before and after November 2013, and thick dashed lines indicate that linear trends have passed a F-test at 99% significant level.**

444
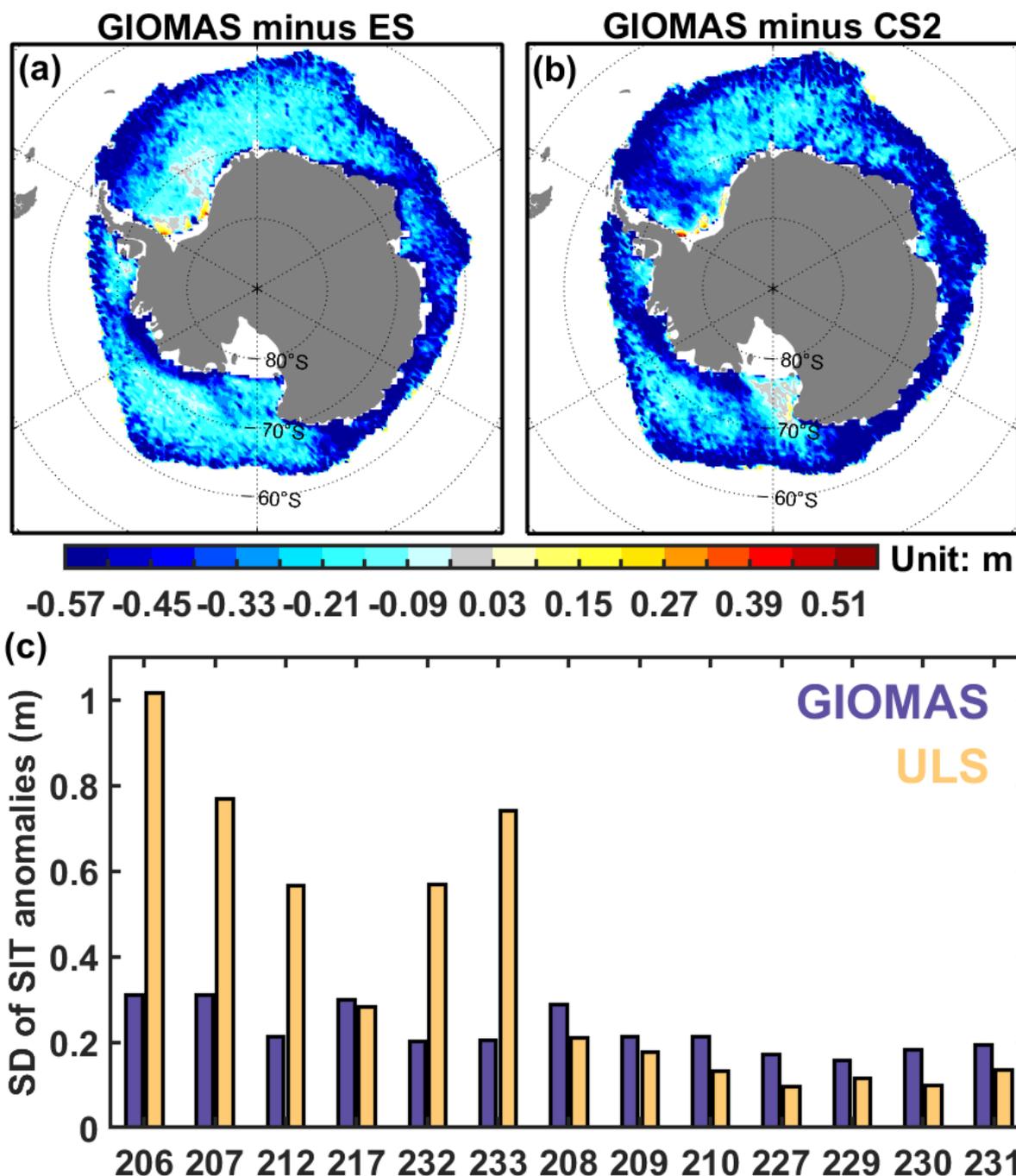
Figure 6: (a) The spatial differences in standard deviation of SIT anomalies between GIOMAS and ES. (b) same as (a) but for differences between GIOMAS and CS2. (c) The standard deviation of SIT anomalies for ULS (yellow) and corresponding GIOMAS (blue).
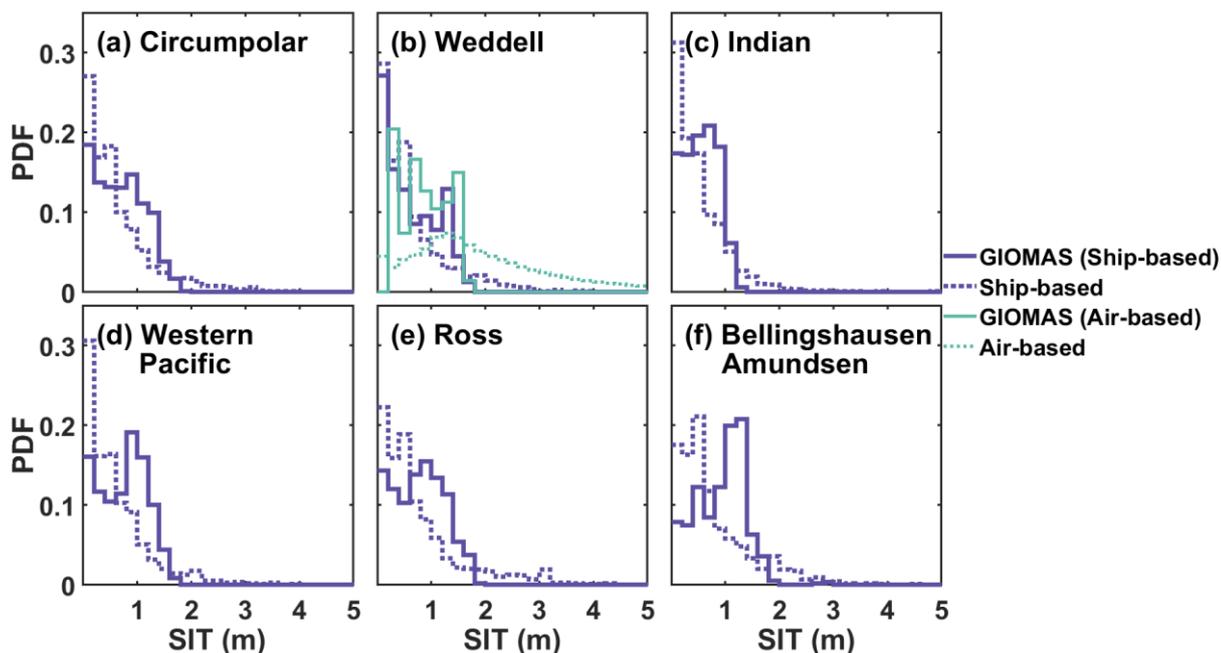
450
451 **Figure 7: SIT histograms of GIOMAS (solid polyline) and in-situ observations (dashed polyline) in (a) the Southern Ocean and (b-**
452 **f) five sectors. The purple and green denote data related to ship-based and air-based observations, respectively.**

453